UC San Diego
UC San Diego Previously Published Works

Title
General Realization Algorithm for Modal Identification of Linear Dynamic Systems

Permalink
https://escholarship.org/uc/item/18b40014

Journal
Journal of Engineering Mechanics, ASCE, 134(9)

ISSN
0733-9399

Authors
De Callafon, Raymond A.
Moaveni, Babak
Conte, Joel P
et al.

Publication Date
2008-09-01

DOI
10.1061/(ASCE)0733-9399(2008)134:9(712)

Peer reviewed

eScholarship.org Powered by the California Digital Library
University of California

General Realization Algorithm for Modal Identification of Linear Dynamic Systems

R. A. De Callafon[1], B. Moaveni[2], J. P. Conte[3], M. ASCE, X. He[4], and E. Udd[5]

ABSTRACT:

The General Realization Algorithm (GRA) is developed to identify modal parameters of linear multi-degree-of-freedom dynamic systems subjected to measured (known) arbitrary dynamic loading from known initial conditions. The GRA extends the well known Eigensystem Realization Algorithm (ERA) based on Hankel matrix decomposition by allowing an arbitrary input signal in the realization algorithm. This generalization is obtained by performing a weighted Hankel matrix decomposition, where the weighting is determined by the loading. The state-space matrices are identified in a two-step procedure that includes a state reconstruction followed by a least squares optimization to get the minimum prediction error for the response. The statistical properties (i.e., bias, variance, and robustness to added output noise introduced to model measurement noise and modeling errors) of the modal parameter estimators provided by the GRA are investigated through numerical simulation based on a benchmark problem with non-classical damping.

CE Database subject headings: System identification; Modal analysis; Modal parameters; Linear systems; Earthquake excitation.

Introduction

As the performance of computational algorithms and computers have drastically increased, the problem of identifying the properties and conditions of structures from their measured response to an external excita-

1. Associate Professor, Dept. of Mechanical and Aerospace Engineering, University of California at San Diego, 9500 Gilman Drive, La Jolla, California 92093-0085; E-mail: callafon@ucsd.edu
2. Post doctoral researcher, Dept. of Structural Engineering, University of California at San Diego, 9500 Gilman Drive, La Jolla, California 92093-0085; E-mail: bmoaveni@ucsd.edu
3. Professor, Dept. of Structural Engineering, University of California at San Diego, 9500 Gilman Drive, La Jolla, California 92093-0085; E-mail: jpconte@ucsd.edu (corresponding author)
4. Post doctoral researcher, Dept. of Structural Engineering, University of California at San Diego, 9500 Gilman Drive, La Jolla, California 92093-0085; E-mail: x1he@ucsd.edu
5. Columbia Gorge Research, 2555 NE 205th Avenue, Fairview, Oregon 97024; E-mail: ericudd@aol.com

tion has received considerable attention. There has been a vast number of studies and algorithms concerning the construction of state-space representations of linear dynamic systems in the time domain, starting with the work of Gilbert (1963) and Kalman (1963). One of the first important results in this field is about minimal state-space realization, indicating a model with the smallest state-space dimension among realized systems that have the same input-output relations within a specified degree of accuracy (Juang and Pappa 1985). It was shown by Ho and Kalman (1965) that the minimum representation problem is equivalent to the problem of identifying the sequence of real matrices, known as the Markov parameters, which represent the impulse response of a linear dynamic system. Numerous studies (Silverman 1971, Phan et al. 1991) have been conducted on the subject of Markov parameters and their relations to different representations of linear dynamic systems.

Following a time-domain formulation and incorporating results from control theory, Juang and Pappa (1985) proposed the Eigensystem Realization Algorithm (ERA) for modal parameter identification and model reduction of linear dynamic systems. ERA extends the Ho-Kalman algorithm and creates a minimal realization that mimics the output history of the system when it is subjected to a unit pulse input. Later, this algorithm was refined to better handle the effects of noise and structural nonlinearities, and ERA with data correlations (ERA/DC) was proposed (Juang et al. 1988). The Natural Excitation Technique combined with ERA (NExT-ERA), first proposed by James et al. (1993), is based on the same idea as ERA/DC in order to identify the modal parameters of a system using output-only ambient vibration data. Peeters and De Roeck (2001) reviewed several output-only system identification methods which are useful for operational modal analysis under the condition that the input excitation is broadband (ideally white noise). Although these methods are powerful in generating dynamic models from impulse response and/or ambient vibration data, realization algorithms similar to ERA that can handle arbitrary input signals are needed. For arbitrary input signal, identification methods based on prediction error minimization (Ljung 1999) or subspace methods (Van Overschee and De Moore 1996) can be used. Unfortunately, prediction error methods require an intricate model parametrization, specially for multivariable systems, along with a nonlinear

optimization to identify model parameters. These issues have been resolved in subspace based identification, but the link with direct realization algorithms is not transparent. This paper establishes a straightforward extension of the well-known eigensystem realization algorithm, by development of the General Realization Algorithm (GRA) on the basis of an arbitrary input signal.

The proposed GRA allows for the realization of a state-space model on the basis of input-output measurement data using a Hankel matrix based realization algorithm similar to the well-known ERA. GRA allows for an explicit use of the input signal through construction of a so-called weighted Hankel matrix from the input-output measurements. In the special case where the input excitation is an impulse signal, GRA reduces down to ERA in which a Hankel matrix is formed on the basis of impulse (free vibration) response measurements. The explicit use of the input signal to construct the weighted Hankel matrix in GRA shows an advantage in comparison to the case where only Markov parameter estimates are used to initiate a standard Hankel matrix based realization as in ERA. This advantage is more significant when the input excitation is a short-duration and/or non-broadband (colored) signal such as earthquake ground motions.

In this paper, the GRA is presented to identify the dynamic characteristics of linear multi-degree-of-freedom dynamic systems subjected to arbitrary loading from zero (at rest) or known non-zero initial conditions. The identified state-space matrices are improved by a least squares algorithm, upon state reconstruction, to get the minimum prediction error for the response. Statistical properties (i.e., bias, variance, and robustness to added output noise) of the modal parameter estimators provided by the GRA are investigated through a numerical simulation study based on a benchmark problem with non-classical damping.

Eigensystem Realization Algorithm (ERA)

In order to present clearly the foundation of the General Realization Algorithm (GRA) for arbitrary input signals, first the Eigensystem Realization Algorithm (ERA) for pulse input signal is briefly reviewed in this section; more details can be found in Juang and Pappa (1985). In the next section, ERA is generalized

for arbitrary input signals, which often characterize the input excitation of actual dynamic systems (e.g., seismic excitation of a bridge or building structure).

Consider a P degree-of-freedom (DOF) linear dynamic system represented in state-space form at discrete times $t = k\,\Delta T$, $k = 0, 1, 2, ...$, with a constant sampling time ΔT, as

$$\begin{aligned} \mathbf{x}(k+1) &= \mathbf{A}\mathbf{x}(k) + \mathbf{B}\mathbf{u}(k) \\ \mathbf{y}(k) &= \mathbf{C}\mathbf{x}(k) + \mathbf{D}\mathbf{u}(k) \end{aligned} \tag{1}$$

in which $\mathbf{x}(k) \in \mathbb{R}^{n \times 1}$ ($n = 2P$) denotes an n-dimensional state vector, state matrix $\mathbf{A} \in \mathbb{R}^{n \times n}$, input matrix $\mathbf{B} \in \mathbb{R}^{n \times r}$, output matrix $\mathbf{C} \in \mathbb{R}^{m \times n}$ and feed-through matrix $\mathbf{D} \in \mathbb{R}^{m \times r}$ completely define a linear dynamic system with an r-dimensional forcing function, $\mathbf{u}(k)$, and m-dimensional output measurement, $\mathbf{y}(k)$. To simplify notations, the discrete time impulse response measurements, $\mathbf{g}(k)$, (also referred to as Markov parameters for unit pulse input), are assumed to be vector valued (i.e., single input, multiple output system). The formulation of ERA can be generalized to multiple input - multiple output systems (Juang and Pappa 1985) that is avoided here in order to focus on the main concepts.

Given the discrete time state-space model of a linear dynamic system, as in Eq. (1), the output $\mathbf{y}(k)$ due to the arbitrary input signal $\mathrm{u}(k)$ can be written explicitly as

$$\mathbf{y}(k) = \mathbf{D}\mathrm{u}(k) + \sum_{i=1}^{\infty} \mathbf{g}(i)\mathrm{u}(k-i), \qquad \mathbf{g}(i) = \mathbf{C}\mathbf{A}^{i-1}\mathbf{B} \tag{2}$$

where $\mathbf{g}(i)$ denote the Markov parameters, and k indicates the input and output samples at discrete times $t = k\,\Delta T$, ($k = 0, 1, ..., 2N$). Given the discrete output measurements $\mathbf{y}(k)$ and possibly the input measurements $\mathrm{u}(k)$ for $k = 0, 1, 2, ..., 2N$, the objective is to determine the appropriate size n (McMillan degree) of the state vector $\mathbf{x}(k)$ in Eq. (1) (i.e., order of the model to realize), and to estimate a discrete time state-space realization ($\mathbf{A}$, $\mathbf{B}$, $\mathbf{C}$, $\mathbf{D}$) of the dynamic system considered.

For the special case of a unit pulse input, the output $\mathbf{y}(k)$ corresponds to the Markov parameters, $\mathbf{g}(k)$, of the discrete time system. To set up the realization algorithm on the basis of the impulse response measurements, $\mathbf{g}(k) = \mathbf{y}(k)$ ($k = 0, 1, 2, ..., 2N$), first an $(m \times N) \times N$ Hankel matrix $\mathbf{H}$ is constructed as

$$\mathbf{H} = \begin{bmatrix} \mathbf{g}(1) & \mathbf{g}(2) & \dots & \mathbf{g}(N) \\ \mathbf{g}(2) & \mathbf{g}(3) & \dots & \mathbf{g}(N+1) \\ \dots & \dots & \dots & \dots \\ \mathbf{g}(N) & \mathbf{g}(N+1) & \dots & \mathbf{g}(2N-1) \end{bmatrix}_{(m \times N) \times N} \tag{3}$$

and a corresponding shifted Hankel matrix $\overline{\mathbf{H}}$ of the same size is defined as

$$\overline{\mathbf{H}} = \begin{bmatrix} \mathbf{g}(2) & \mathbf{g}(3) & \dots & \mathbf{g}(N+1) \\ \mathbf{g}(3) & \mathbf{g}(4) & \dots & \mathbf{g}(N+2) \\ \dots & \dots & \dots & \dots \\ \mathbf{g}(N+1) & \mathbf{g}(N+2) & \dots & \mathbf{g}(2N) \end{bmatrix}_{(m \times N) \times N} \tag{4}$$

In case $\mathbf{g}(k)$ are noise free impulse response, it follows that

$$\mathbf{g}(k) = \begin{cases} \mathbf{D}, & \text{for } k = 0 \\ \mathbf{C}\mathbf{A}^{k-1}\mathbf{B}, & \text{for } k \geq 0 \end{cases} \tag{5}$$

The Hankel matrix $\mathbf{H}$ in Eq. (3) can be expressed as

$$\mathbf{H} = \mathbf{H}_1\mathbf{H}_2 \tag{6}$$

in which $\mathbf{H}_1$ and $\mathbf{H}_2$ are the observability and controllability matrices, respectively,

$$\mathbf{H}_1 = \begin{bmatrix} \mathbf{C} \\ \mathbf{C}\mathbf{A} \\ \mathbf{C}\mathbf{A}^2 \\ \dots \\ \mathbf{C}\mathbf{A}^{N-1} \end{bmatrix}_{(m \times N) \times n} \quad \text{and} \quad \mathbf{H}_2 = \begin{bmatrix} \mathbf{B} & \mathbf{A}\mathbf{B} & \mathbf{A}^2\mathbf{B} & \dots & \mathbf{A}^{N-1}\mathbf{B} \end{bmatrix}_{n \times N} \tag{7}$$

For a discrete time state-space model, Eq. (1), of order (or McMillan degree) n, it can be shown via the Cayley-Hamilton theorem that both $\mathbf{H}_1$ and $\mathbf{H}_2$ have full column rank n and full row rank n, respectively. As a result, the Hankel matrix $\mathbf{H}$ has rank n. Furthermore, from its definition, the shifted Hankel matrix $\overline{\mathbf{H}}$ can be shown to have the following shift property:

$$\bar{\mathbf{H}} = \mathbf{H}_1 \mathbf{A} \mathbf{H}_2 \tag{8}$$

where $\mathbf{H}_1$ and $\mathbf{H}_2$ are as defined as in Eq. (7). As both $\mathbf{H}_1$ and $\mathbf{H}_2$ have respectively full column and row rank n, there exists a left inverse $\mathbf{H}_1^{\dagger}$ and a right inverse $\mathbf{H}_2^{\dagger}$ such that

$$\mathbf{H}_1^{\dagger}\mathbf{H}_1 = \mathbf{I}_{n \times n} \qquad \text{and} \qquad \mathbf{H}_2\mathbf{H}_2^{\dagger} = \mathbf{I}_{n \times n} \tag{9}$$

so that, from Eq. (8),

$$\mathbf{A} = \mathbf{H}_1^{\dagger}\, \bar{\mathbf{H}} \mathbf{H}_2^{\dagger} \tag{10}$$

The above left and right inverses are obtained as

$$\begin{aligned} \mathbf{H}_1^{\dagger} &= [\mathbf{H}_1^{\mathrm{T}}\mathbf{H}_1]^{-1}\mathbf{H}_1^{\mathrm{T}} \\ \mathbf{H}_2^{\dagger} &= \mathbf{H}_2^{\mathrm{T}}[\mathbf{H}_2\mathbf{H}_2^{\mathrm{T}}]^{-1} \end{aligned} \tag{11}$$

During the identification process, the decomposition of $\mathbf{H}$ into $\mathbf{H}_1$ and $\mathbf{H}_2$ according to Eq. (6) can be performed through a singular value decomposition (SVD), $\mathbf{H} = \mathbf{U}\boldsymbol{\Sigma}\mathbf{V}^{\mathrm{T}}$, where both $\mathbf{U}$ and $\mathbf{V}$ are orthonormal matrices and $\boldsymbol{\Sigma}$ is a diagonal matrix with the (non-negative) singular values ordered in decreasing magnitude on the main diagonal. The SVD provides insight into the rank of $\mathbf{H}$ (Vandewalle and de Moor 1991), as the rank of $\mathbf{H}$ is given by the number of non-zero diagonal elements (singular values) in $\boldsymbol{\Sigma}$ for the case of noise free measurements. In the case where the rank of $\mathbf{H}$ is significantly larger than n (due to the presence of measurement noise), a decision can be made regarding the order n of the system (or effective rank of the Hankel matrix $\mathbf{H}$) on the basis of the plot of the singular values. In this case, the SVD allows to approximate the high rank Hankel matrix $\mathbf{H}$ into a lower rank (n) matrix via a separation of large and small singular values of matrix $\mathbf{H}$. The use of SVD to compute a low rank decomposition of the Hankel matrix is essential in the realization method and has been used in the classical Kung's realization algorithm (Kung 1978) as well as in ERA (Juang and Pappa 1985). The SVD of the Hankel matrix $\mathbf{H}$ can be expressed as

$$\mathbf{H} = \mathbf{U}\boldsymbol{\Sigma}\mathbf{V}^{\mathrm{T}} = \begin{bmatrix}\mathbf{U}_n & \mathbf{U}_s\end{bmatrix}\begin{bmatrix}\boldsymbol{\Sigma}_n & \mathbf{0} \\ \mathbf{0} & \boldsymbol{\Sigma}_s\end{bmatrix}\begin{bmatrix}\mathbf{V}_n^{\mathrm{T}} \\ \mathbf{V}_s^{\mathrm{T}}\end{bmatrix} \tag{12}$$

in which $\boldsymbol{\Sigma}$ is split up in the two diagonal matrices $\boldsymbol{\Sigma}_n$ and $\boldsymbol{\Sigma}_s$, where $\boldsymbol{\Sigma}_s$ and $\boldsymbol{\Sigma}_n$ denote the part of $\boldsymbol{\Sigma}$ with the s small (zero in the case of noise free measurements) singular values and the part of $\boldsymbol{\Sigma}$ with the n large (non-zero in the case of noise free measurements) singular values, respectively. As already mentioned above, a decision on an appropriate value of the rank n of the reduced-rank Hankel matrix can be made by plotting the singular values.

Using the partitioned SVD in Eq. (12), the high rank Hankel matrix $\mathbf{H}$ can be approximated by a reduced rank n matrix $\mathbf{H}_n$ of the same dimension as

$$\mathbf{H}_n = \mathbf{U}_n \Sigma_n \mathbf{V}_n^{\mathrm{T}} \tag{13}$$

which can be shown to minimize $\|\mathbf{H} - \mathbf{H}_n\|_2$ where $\| \ldots \|_2$ denotes the induced two-norm or maximum singular value of a matrix. On the basis of the above rank n decomposition, the matrices $\mathbf{H}_1$ and $\mathbf{H}_2$ in Eq. (6) can be estimated as

$$\begin{aligned}\mathbf{H}_1 &= \mathbf{U}_n \boldsymbol{\Sigma}_n^{1/2} \\ \mathbf{H}_2 &= \boldsymbol{\Sigma}_n^{1/2} \mathbf{V}_n^{\mathrm{T}}\end{aligned} \tag{14}$$

from which the expressions for the left inverse $\mathbf{H}_1^{\dagger}$ and right inverse $\mathbf{H}_2^{\dagger}$ simplify to

$$\begin{aligned}\mathbf{H}_1^{\dagger} &= \boldsymbol{\Sigma}_n^{-1/2} \mathbf{U}_n^{\mathrm{T}} \\ \mathbf{H}_2^{\dagger} &= \mathbf{V}_n \boldsymbol{\Sigma}_n^{-1/2}\end{aligned} \tag{15}$$

From the results in Eqs. (13) through (15) and using Eqs. (5), (7) and (10), it follows that the state-space matrices of the discrete time model in Eq. (1) are given by

$$\mathbf{D} = \mathbf{g}(0), \quad \mathbf{C} = \mathbf{H}_1(1{:}m, :), \quad \mathbf{B} = \mathbf{H}_2(:, 1) \quad \text{and} \quad \mathbf{A} = \mathbf{H}_1^{\dagger}\overline{\mathbf{H}}\mathbf{H}_2^{\dagger} \tag{16}$$

where the notations (1:m , :) and (: , 1) denote the first m rows and the first column of a matrix, respectively. It should be noted that ERA is also readily applicable to free vibration response data. In this case, the Hankel matrix is constructed using free vibration data (i.e., $\mathbf{y}(0)$ as first element of the Hankel matrix), and the identified input matrix $\mathbf{B}$ represents the non-zero initial state $\mathbf{x}_0$, which is related to the initial nodal displacements and velocities in the physical state $\bar{\mathbf{x}}_0$ through the linear transformation $\bar{\mathbf{x}}_0 = \mathbf{T}\mathbf{x}_0$.

General Realization Algorithm (GRA)

As discussed in the previous section, ERA assumes either a pulse input signal or free vibration response to construct the Hankel matrix. In many practical situations, the dynamic excitation acts over a finite-time or continually and the dynamic response of the structure during forced vibration contains valuable information on the system dynamics. Unfortunately, ERA cannot incorporate this information directly. The objective of this section is to extend ERA to accommodate arbitrary excitation signals.

Although ERA is not directly applicable to general excitation signals, estimates of the Markov parameters can be obtained separately and fed into ERA. Such an estimation can be achieved via (i) non-parametric estimation methods such as correlation analysis, e.g., NExT-ERA by James et al. (1993), (ii) estimation of a Finite Impulse Response (FIR) model, e.g., Oppenheim and Schafer (1989), (iii) inverse Fourier transformation of an empirical transfer function estimate, e.g., Ljung (1999), or (iv) wavelet transformation, e.g., Alvin et al. (2003). Unfortunately, for accurate estimation of the Markov parameters, these methods require a broadband excitation signal u(k). A narrow band excitation will lead to biased and noisy (large variance) estimation of the Markov parameters that will in turn pollute the results of the subsequent application of ERA. An alternative would be to reconstruct the Markov parameters from a Kalman filter or other state observer, as done in Phan et al. (1992). Although this is a powerful method, it requires relatively long input-output data in the least squares procedure used to compute the Markov parameters (Lus et al.

2002). The method presented below aims at estimating the dynamic properties of the structure based on a (short-time) input-output data sequence available.

To illustrate the main idea behind GRA, consider the discrete time input-output relationship given in Eq. (2) that can be rewritten in the following Hankel matrix based representation

$$\mathbf{Y} = \mathbf{HU} + \mathbf{E} \tag{17}$$

where **H** is the truncated (the first i block rows with $i < N$) Hankel matrix given in Eq. (3) and

$$\mathbf{Y} = \begin{bmatrix} \mathbf{y}(1) & \mathbf{y}(2) & \dots & \mathbf{y}(N) \\ \mathbf{y}(2) & \mathbf{y}(3) & \dots & \mathbf{y}(N+1) \\ \dots & \dots & \dots & \dots \\ \mathbf{y}(i) & \mathbf{y}(i+1) & \dots & \mathbf{y}(i+N-1) \end{bmatrix}_{(m \times i) \times N}, \qquad \mathbf{U} = \begin{bmatrix} \mathrm{u}(0) & \mathrm{u}(1) & \dots & \mathrm{u}(N-1) \\ 0 & \mathrm{u}(0) & \dots & \mathrm{u}(N-2) \\ \dots & \dots & \dots & \dots \\ 0 & 0 & \dots & \mathrm{u}(0) \end{bmatrix}_{N \times N},$$

$$\mathbf{E} = \begin{bmatrix} \mathbf{g}(0)\mathrm{u}(1) & \mathbf{g}(0)\mathrm{u}(2) & \dots & \mathbf{g}(0)\mathrm{u}(N) \\ \mathbf{g}(0)\mathrm{u}(2) + \mathbf{g}(1)\mathrm{u}(1) & \mathbf{g}(0)\mathrm{u}(3) + \mathbf{g}(1)\mathrm{u}(2) & \dots & \mathbf{g}(0)\mathrm{u}(N+1) + \mathbf{g}(1)\mathrm{u}(N) \\ \dots & \dots & \dots & \dots \\ \sum_{l=0}^{i-1} \mathbf{g}(l)\mathrm{u}(i-l) & \sum_{l=0}^{i-1} \mathbf{g}(l)\mathrm{u}(i-l+1) & \dots & \sum_{l=0}^{i-1} \mathbf{g}(l)\mathrm{u}(i+N-l-1) \end{bmatrix}_{(m \times i) \times N} \tag{18}$$

In the above equation, **H** is the conventional Hankel matrix of impulse response coefficients $\mathbf{g}(k)$ and **Y** is a Hankel matrix consisting of the measured output data due to the (arbitrary) input $\mathrm{u}(k)$. The input data is stored in the $N \times N$ square matrix **U**, which is non-singular provided that $\mathrm{u}(0) \neq 0$. It is observed from Eqs. (17) and (18) that matrix **E** contains terms defined as the sum of input signals weighted by the corresponding Markov parameters, which can be estimated from input-output data. To show this, consider the input measurement u(0), which corresponds to the start of the non-zero input signal during the experiment, to be normalized to u(0) = 1 without loss of generality (i.e., both the input u and the output **y** are scaled by the same factor, namely the original/unscaled value of u(0)). This greatly simplifies the formulation and with $\mathrm{u}(k) = 0$ for $k < 0$, $\mathbf{g}(l)$ can be computed recursively from the input-output data as

$$\mathbf{g}(l) = \mathbf{y}(l) - \sum_{k=0}^{l-1} \mathbf{g}(k)\mathrm{u}(l-k), \qquad \mathbf{g}(0) = \mathbf{y}(0) \tag{19}$$

which is equivalent to

$$\mathbf{G}_N = \mathbf{Y}_N \cdot \mathbf{U}^{-1} \tag{20}$$

where **U** is given in Eq. (18) with u(0) = 1, and

$$\mathbf{Y}_N = \left[\mathbf{y}(0)\ \ \mathbf{y}(1)\ \ \ldots\ \ \mathbf{y}(N-1)\right]_{m \times N} \quad \text{and} \quad \mathbf{G}_N = \left[\mathbf{g}(0)\ \ \mathbf{g}(1)\ \ \ldots\ \ \mathbf{g}(N-1)\right]_{m \times N} \tag{21}$$

Although matrix **U** is an upper triangular matrix with a determinant of one, this matrix can be ill-conditioned, especially for a large number of data points *N*. Numerically, is it advantageous to replace Eq. (20) by

$$\mathbf{G}_N = \mathbf{Y}_N \cdot \mathbf{U}^{\dagger} \tag{22}$$

where $\mathbf{U}^{\dagger}$ is the Moore-Penrose pseudo-inverse (Noble and Daniel, 1988) of **U** with a tolerance on the singular values considered in computing this matrix. It should be noted that the impulse response estimate (or Markov parameter estimates) can also be obtained using different methods than the one shown in Eq. (22). Some of these methods such as Observer/Kalman filter identification (Phan et al. 1991) can be used to estimate Markov parameters without requiring knowledge of the initial conditions. The impulse response estimates are then used to compute the elements of matrix **E** which can be calculated as

$$\mathbf{E}(i, k) = \sum_{l=0}^{i-1} \mathbf{G}_N(l+1)\mathrm{u}(k+i-l-1) \tag{23}$$

where $\mathbf{E}(i, k)$ denotes the kth column of ith block row of matrix **E** and $\mathbf{G}_N(l+1)$ is the $(l+1)^{\text{th}}$ column of $\mathbf{G}_N$ matrix given in Eq. (22). In the case of noisy measurements $\mathbf{Y}_N$, the variance of $\mathbf{G}_N(l)$ increases with *l*. It can be observed from Eq. (23) that increasingly values of *l* in $\mathbf{G}_N(l)$ are needed to compute the successive block rows of the matrix **E**. To mitigate the effects of the increasing variance (as a function of *l*) of the impulse response estimates $\mathbf{G}_N(l)$, a limited number *i* $(n \le i < N)$ of block rows of matrix **E** of dimension $(m \times i) \times N$ is used such that $\mathbf{G}_N(i)$ has a reasonably small variance. In the previous statement, *N* denoted the total number of data points minus *i*, and *n* is the anticipated order of the model to be estimated. Defining $\mathbf{R} = \mathbf{Y} - \mathbf{E} = \mathbf{HU}$ as a weighted Hankel matrix, it follows from the full rank prop-

erty of **U** that rank (**H**) = rank (**R**). In the case of noise free measurements, rank (**R**) is equal to the exact order of the system to be identified. GRA allows a state-space realization of the system directly on the basis of the weighted Hankel matrix **R**, from which the modal parameters of the system can be obtained. Alternatively to the above, matrix **H** could be computed via $\mathbf{H} = \mathbf{R}\mathbf{U}^{-1}$ (or $\mathbf{H} = \mathbf{R}\mathbf{U}^{\dagger}$), but that would require an additional inverse (or pseudo-inverse) of the possibly ill-conditioned matrix **U** which would result in large variances of the high column entries of the Hankel matrix **H**.

To continue the development of GRA, a lower rank decomposition via SVD is applied to **R** as

$$\mathbf{R} = \mathbf{U}\boldsymbol{\Sigma}\mathbf{V}^{\mathrm{T}} = \begin{bmatrix}\mathbf{U}_n & \mathbf{U}_s\end{bmatrix}\begin{bmatrix}\boldsymbol{\Sigma}_n & \mathbf{0} \\ \mathbf{0} & \boldsymbol{\Sigma}_s\end{bmatrix}\begin{bmatrix}\mathbf{V}_n^{\mathrm{T}} \\ \mathbf{V}_s^{\mathrm{T}}\end{bmatrix} \tag{24}$$

which is similar to Eq. (12) for Hankel matrix **H**. Using this SVD decomposition, matrix **R** can be approximated by a rank n matrix $\mathbf{R}_n$ of the same dimensions as

$$\mathbf{R}_n = \mathbf{U}_n\boldsymbol{\Sigma}_n\mathbf{V}_n^{\mathrm{T}} \tag{25}$$

which can be shown to minimize $\|\mathbf{R} - \mathbf{R}_n\|_2$. Therefore, $\mathbf{R}_n$ can be factorized as

$$\mathbf{R}_n = \mathbf{R}_1\mathbf{R}_2 \tag{26}$$

in which

$$\begin{aligned}\mathbf{R}_1 &= \mathbf{U}_n\boldsymbol{\Sigma}_n^{1/2} \\ \mathbf{R}_2 &= \boldsymbol{\Sigma}_n^{1/2}\mathbf{V}_n^{\mathrm{T}}\end{aligned} \tag{27}$$

Similar to Hankel matrix $\mathbf{H}$ in Eq. (8), matrix **R** has the shift property

$$\overline{\mathbf{R}} = \mathbf{R}_1\mathbf{A}\mathbf{R}_2 \tag{28}$$

where $\overline{\mathbf{R}} = \overline{\mathbf{Y}} - \overline{\mathbf{E}}$ in which shifted matrix $\overline{\mathbf{Y}}$ is defined similar to $\overline{\mathbf{H}}$ in Eq. (4) and $\overline{\mathbf{E}}$ is given by

$$\bar{\mathbf{E}} = \begin{bmatrix} \mathbf{g}(0)\mathrm{u}(2) + \mathbf{g}(1)\mathrm{u}(1) & \mathbf{g}(0)\mathrm{u}(3) + \mathbf{g}(1)\mathrm{u}(2) & \dots & \mathbf{g}(0)\mathrm{u}(N+1) + \mathbf{g}(1)\mathrm{u}(N) \\ \dots & \dots & \dots & \dots \\ \sum_{l=0}^{i} \mathbf{g}(l)\mathrm{u}(i+1-l) & \sum_{l=0}^{i} \mathbf{g}(l)\mathrm{u}(i-l+2) & \dots & \sum_{l=0}^{i} \mathbf{g}(l)\mathrm{u}(i+N-l-1) \end{bmatrix}_{(m \times i) \times N} \tag{29}$$

From the above properties of matrix $\mathbf{R}$, it follows that a realization based algorithm similar to ERA based on the input-output data matrices $\mathbf{R}$ and $\bar{\mathbf{R}}$ can be used to construct the discrete time state-space matrices in Eq. (1) for the case of arbitrary input u(k). This is achieved simply by replacing $\mathbf{H}$ by $\mathbf{R}$ in Eq. (16).

The main idea behind GRA is to use the information of the input signal to create a weighted Hankel matrix $\mathbf{R} = \mathbf{Y} - \mathbf{E} = \mathbf{HU}$, instead of creating a (unweighted) Hankel matrix **H** by first estimating a large number of Markov parameters on the basis of a short-time and/or non-white input sequence. In the application of GRA, the Markov parameter estimates are used to build up the error matrix **E**, which in turn is used to create the weighted Hankel matrix **R** on which a realization algorithm is performed to compute a state-space model. However, by carefully examining the formula and size of matrix **E**, it is observed that only a small number of Markov parameter estimates is needed to create a “large fat” (very high number of columns compared to the number of block-rows) matrix **E** and consequently matrix $\mathbf{R} = \mathbf{Y} - \mathbf{E}$. Therefore, the use of a “large fat” unweighted Hankel matrix **H** for which a large number of Markov parameters would be required, is avoided. In other words, as compared to ERA, the proposed GRA reduces the required length of the Markov parameter sequence to obtain accurate system identification results.

To show that GRA is a generalization of ERA, it can be seen that for a unit pulse input u(k), matrix **U** becomes the $N \times N$ identity matrix, while matrix **E** becomes a $(m \times i) \times N$ zero matrix since u(k) = 0 for $k \neq 0$. In another special case where the input signal u(k) is the unit step which is typically applied to flexible mechanical (servo) systems in order to study their transient dynamic behavior, matrix **U** is an upper triangular matrix and matrix **E** is a row-wise listing of output signals as

$$\mathbf{U} = \begin{bmatrix} 1 & 1 & \dots & 1 \\ 0 & 1 & \dots & 1 \\ \dots & \dots & \dots & \dots \\ 0 & 0 & \dots & 1 \end{bmatrix}_{N \times N}, \qquad \mathbf{E} = \begin{bmatrix} \mathbf{y}(0) & \mathbf{y}(0) & \dots & \mathbf{y}(0) \\ \mathbf{y}(1) & \mathbf{y}(1) & \dots & \mathbf{y}(1) \\ \dots & \dots & \dots & \dots \\ \mathbf{y}(i-1) & \mathbf{y}(i-1) & \dots & \mathbf{y}(i-1) \end{bmatrix}_{(m \times i) \times N} \tag{30}$$

as previously shown by de Callafon (2003). In the latter case, applying GRA to matrix **R** which depends only on step response data yields significantly better results in terms of system realization than applying ERA based on impulse response data obtained through differentiating the step response measurements (de Callafon 2003).

Refinement of State-Space Realization through Least Squares Optimization

Although Eq. (16) allows to identify the state-space matrices **A**, **B** and **C** based on the SVD of a high-dimensional Hankel matrix both for ERA and GRA, the feed-through matrix **D** is estimated from the single, possibly noisy, measurement $\mathbf{g}(0)$. Using the estimates of the state matrix **A** and the input matrix **B** obtained through ERA or GRA, the state vector $\mathbf{x}(k)$ can be reconstructed as

$$\mathbf{x}(k+1) = \mathbf{A}\mathbf{x}(k) + \mathbf{B}\mathrm{u}(k), \qquad \mathbf{x}(0) = \mathbf{0} \tag{31}$$

for $k = 0, 1, ..., 2N$. With the reconstructed state vector $\mathbf{x}(k)$, the realization algorithm (ERA or GRA) that is used to compute matrices **A** and **B** can be followed by a standard Least Squares (LS) optimization problem to improve the estimation of the state-space matrices. The LS problem can be stated by rewriting Eq. (1) and adding the zero mean noise vector $\mathbf{V}(k)$ as

$$\mathbf{Y}(k) = \mathbf{\Theta}\mathbf{U}(k) + \mathbf{V}(k), \qquad k = 1, \dots, 2N \tag{32}$$

where

$$\mathbf{Y}(k) = \begin{bmatrix} \mathbf{x}(k+1) \\ \mathbf{y}(k) \end{bmatrix}, \quad \mathbf{\Theta} = \begin{bmatrix} \mathbf{A} & \mathbf{B} \\ \mathbf{C} & \mathbf{D} \end{bmatrix}, \quad \mathbf{U}(k) = \begin{bmatrix} \mathbf{x}(k) \\ \mathrm{u}(k) \end{bmatrix} \quad \text{and} \quad \mathbf{V}(k) = \begin{bmatrix} \mathbf{w}(k) \\ \mathbf{v}(k) \end{bmatrix} \tag{33}$$

in which $\mathbf{w}(k)$ represents the possible noise on the reconstructed state vector $\mathbf{x}(k)$ and $\mathbf{v}(k)$ the noise on the measured output $\mathbf{y}(k)$ which includes measurement noise. Noise vector $\mathbf{V}(k)$ could also include the effects

of parameter estimation errors and modeling error. Including all input-output data for $k = 1, ..., 2N$ in a single matrix representation, Eq. (32) can be rewritten as

$$\mathbf{Y} = \mathbf{\Theta U} + \mathbf{V}, \quad \mathbf{Y} = \left[\mathbf{Y}(0)\ \mathbf{Y}(1)\ \ldots\ \mathbf{Y}(2N)\right], \quad \mathbf{U} = \left[\mathbf{U}(0)\ \mathbf{U}(1)\ \ldots\ \mathbf{U}(2N)\right] \tag{34}$$

Then the state-space matrices in $\mathbf{\Theta}$ can be updated via a standard least squares solution as

$$\hat{\mathbf{\Theta}}_{\mathrm{LS}}^{N} = \mathbf{YU}^{\mathrm{T}}[\mathbf{UU}^{\mathrm{T}}]^{-1} \tag{35}$$

provided that matrix **U** has full row rank. The full row rank condition of matrix **U** is related to the input excitation $\mathrm{u}(k)$ and is trivially satisfied for broad-band forcing function (e.g., pulse/impact load, earthquake ground excitation). The least squares improvement renders the estimated state-space matrices less sensitive to noise. If the input u(k) and the reconstructed state $\mathbf{x}(k)$ are uncorrelated with the state noise $\mathbf{w}(k)$ and the measurement noise $\mathbf{v}(k)$, i.e., $\lim_{N \to \infty} (1/N) \times \mathbf{VU}^{\mathrm{T}} = 0$, consistent estimates of the state-space matrices are obtained. This condition is satisfied asymptotically as $N \to \infty$ provided that the experiments are conducted in such a way that the input excitation is uncorrelated with the measurement noise.

Numerical Validation

Definition of Benchmark Problem

In order to investigate the performance of the proposed GRA, the eight-story linear elastic shear building model shown in Fig. 1 subjected to seismic base excitation is used as a case study. This shear building has a constant floor mass of 625 tons, a constant story stiffness of 10^6 [kN/m], and damping properties represented through the non-classical damping matrix **C** (Veletsos and Ventura 1986). The latter was generated from an assumed configuration of inter-multiple-story viscous dampers installed on the structure (between floors 1 and 4, 2 and 6, and 3 and 8) and is given by

$$\mathbf{C} = 400 \times \begin{bmatrix} 16 & -6 & 0 & -4 & 0 & 0 & 0 & 0 \\ -6 & 15 & -5 & 0 & 0 & -4 & 0 & 0 \\ 0 & -5 & 14 & -5 & 0 & 0 & 0 & -4 \\ -4 & 0 & -5 & 12 & -3 & 0 & 0 & 0 \\ 0 & 0 & 0 & -3 & 6 & -3 & 0 & 0 \\ 0 & -4 & 0 & 0 & -3 & 8 & -1 & 0 \\ 0 & 0 & 0 & 0 & 0 & -1 & 2 & -1 \\ 0 & 0 & -4 & 0 & 0 & 0 & -1 & 5 \end{bmatrix} \quad [\mathrm{kN} \cdot \mathrm{sec/m}] \tag{36}$$

Viscously damped systems that do not satisfy the Caughey-O'Kelly condition (Caughey and O'Kelly 1965) generally have complex-valued natural modes of vibration. Such systems are said to be non-classically or non-proportionally damped. The modal parameters of the shear building model considered here are obtained through solving a complex eigenvalue problem in state-space. The computed natural frequencies and damping ratios are reported in Table 1. It is worth noting that the natural frequencies of a non-classically damped system extracted through eigen-analysis of the state matrix, referred to as pseudo-undamped natural frequencies (Veletsos and Ventura 1986), differ from the corresponding natural frequencies of the associated undamped system. Fig. 2 shows the complex-valued mode shapes of the shear building as rotating vectors in the complex plane called polar plots. The indices on the vectors in each polar plot indicate the DOF number (i.e., floor number). The polar plot representation of a mode shape displays the degree of non-classical damping characteristics of that mode. If the components (or DOFs) of a mode shape are collinear (i.e., in phase or out of phase) in the complex plane, then this mode is classically (or proportionally) damped. The more a mode shape's components are scattered in the complex plane, the more this mode is non-classically damped. Since the higher order mode shapes of the shear building considered here exhibit strong non-classical characteristics (Fig. 2), the real parts of these mode shape components do not remain proportional as the complex vectors rotate, i.e., these (real-valued) mode shapes change continuously within one vibration period. In Fig. 3, the real part of all eight complex mode shapes are plotted at four snapshots with 90 degree phase shifts during a vibration period.

Simulation of Measurement Data

The shear building model is subjected to a horizontal base excitation defined as the strong motion part (2-30 sec) of the Imperial Valley, 1940 earthquake ground motion recorded at the El Centro station (see Fig. 4). The shear building output data used in this study consist of the floor absolute acceleration responses to this earthquake excitation. The differential equations of motion formulated in state-space are integrated via complex modal analysis (Peng and Conte 1998), assuming a piecewise linear forcing function, and using piecewise linear exact integration of the complex-valued first-order modal equations of motion. A constant time increment of $\Delta T = 0.02$ sec is used to integrate the equations of motion. To model measurement noise, zero-mean Gaussian white noise processes are added to the simulated output signals. The reason for considering up to high levels of measurement noise (4% in root-mean-square ratio) is to allow for the higher vibration modes to become more difficult to extract from the data due to decreasing signal-to-noise ratio at higher frequencies, a phenomenon typically seen in real-life applications. The performance (e.g., statistical properties of estimated modal parameters) of the new system identification procedure presented above is investigated under increasing level of noise. For a given floor, the noise level is defined as the ratio (in percent) of the root mean square (RMS) of the added noise process to the RMS of the floor absolute acceleration response (computed over the time interval 2-30 sec). The added noise processes at the various floors are simulated as statistically independent. Fig. 5 compares the added noise realizations of various amplitudes (1%, 2%, 3%, and 4%) to all eight modal components of the noise free roof absolute acceleration response obtained as explained in De Callafon et al. (2007). It is clearly observed that depending on the mode and noise level, the modal absolute acceleration response may be buried in the noise, which renders the corresponding modal parameters difficult to identify.

Application of GRA and Discussion of Results

In order to apply GRA to the seismic input and simulated output data, matrices $\mathbf{E}$ and $\overline{\mathbf{E}}$ of size $(8 \times 40) \times 1400$ are formed based on the whole length of the simulated data (1440 data points) as

described in the Section on General Realization Algorithm. The discrete time state-space matrices are realized and then refined through a least squares optimization as described in the previous sections. Such a refinement step is beneficial especially for the estimation of **C** and **D** matrices and therefore for the mode shape estimates. The identified modal natural frequencies and damping ratios are obtained through eigenanalysis of the estimated discrete time state matrix **A**, while the identified mode shapes are obtained as $\boldsymbol{\psi} = \mathbf{C} \cdot \mathbf{A}$ (De Callafon et al. 2007). The modal parameters (natural frequencies, damping ratios, and mode shapes) of all eight modes of the shear building identified from noise free input-output data are in perfect agreement with the corresponding exact values given in Table 1 and Fig. 3. The statistical properties (bias and variance) of the estimated modal parameters using GRA are investigated as a function of the noise level. For this purpose, a set of 100 identifications was performed at each of nine different noise levels (0%, 0.5%, 1%, 1.5%, 2%, 2.5%, 3%, 3.5%, 4%) for the same noise free input-output data. The added vector (8-DOF) noise processes for the 100 identification trials are simulated as statistically independent. Statistics (mean and mean +/- one standard deviation) of the identified-to-exact natural frequency and damping ratios are shown in Figs. 6 and 7, respectively, as a function of the noise level and for the first six vibration modes. Due to the low contribution of the seventh and eighth modes to the total building response (see Fig. 5) and therefore the very weak signal-to-noise ratio, the modal parameters of these modes cannot be identified at and above the minimum level of added noise considered here (0.5%) as the modal responses are buried in the noise. From Figs. 6 and 7, it is observed that (i) the identified modal frequencies and damping ratios are in very good agreement with their exact counterparts, and (ii) in general both bias and variance of the modal frequency and damping ratio estimators based on GRA increase as a function of the noise level. However, in the particular application, the estimated natural frequencies of the first four modes appear to be quasi unbiased at the noise levels considered, which may be due to the significant contribution of these modes to the total response (see Fig. 5). Comparison of Figs. 6 and 7 shows that both bias and standard deviation of the modal damping ratio estimates are significantly larger than those of the natural frequency estimates, as expected from the system identification literature. To complement Figs.

6 and 7, the cumulative distribution functions of the identified-to-exact natural frequencies and damping ratios are plotted in Figs. 8 and 9, respectively, for 1%, 2%, and 3% noise levels and for the first 6 vibration modes (modes 1, 2, and 3 in the left column and modes 4, 5, and 6 in the right column). Figs. 6 through 9 show that (i) the variance of the estimated modal frequencies and damping ratios is significantly larger for higher modes, and (ii) the estimated modal frequencies and damping ratios are generally more sensitive to the noise level for the higher modes. These two observed trends may be due to the fact that the higher modes contribute less to the total response as shown in Fig. 5. Table 2 provides the statistics (mean, coefficient-of-variation, min, max) of the estimated modal frequencies and damping ratios based on 100 identification trials in the presence of 1% output noise.

The modal assurance criterion (MAC) is used to compare the estimated mode shapes with their exact counterparts at different levels of noise. The MAC value is bounded between 0 and 1, measures the degree of correlation between an estimated mode shape, $\boldsymbol{\psi}_{\text{estimated}}$, and its exact counterpart, $\boldsymbol{\psi}_{\text{exact}}$, (MAC value of 1 for exactly estimated mode shape), and is defined as

$$\text{MAC}(\boldsymbol{\psi}_{\text{estimated}}, \boldsymbol{\psi}_{\text{exact}}) = \frac{\left|\boldsymbol{\psi}^{*}_{\text{estimated}} \cdot \boldsymbol{\psi}_{\text{exact}}\right|^2}{\left|\boldsymbol{\psi}_{\text{estimated}}\right|^2 \cdot \left|\boldsymbol{\psi}_{\text{exact}}\right|^2} \tag{37}$$

where superscript * denotes the complex conjugate transpose. The mean and coefficient-of-variation (cov) of the MAC values between estimated and exact mode shapes based on 100 identification trials are reported in Table 3 for all noise levels considered herein and for the first six modes. From these results, it is observed that (i) the first four mode shapes are identified very accurately even in the presence of high amplitude output noise (4%), and (ii) estimates of the higher mode shapes become less accurate with increasing level of noise.

Conclusions

This paper presents the General Realization Algorithm (GRA), a new system realization algorithm to identify modal parameters of linear dynamic systems based on general input-output data. This algorithm is a generalization of the Eigensystem Realization Algorithm (ERA), which is based on singular value decomposition (SVD) of a Hankel matrix constructed from impulse response or free vibration response data. This generalization is obtained through SVD of a weighted Hankel matrix of input-output data, where the weighting is determined by the loading. Using GRA, the state-space matrices are estimated in a two-step process that includes a state reconstruction followed by a least squares optimization yielding a minimum prediction error for the response. An application example consisting of an 8-story shear building model subjected to earthquake base excitation is used for the multiple purposes of validating the new algorithm, evaluating its performance, and investigating the statistical properties (i.e., bias/unbias, variance, and robustness to added output noise introduced to model measurement noise and modeling errors) of the GRA modal parameter estimates. Based on the extensive simulation study performed, it is found that the proposed new algorithm yields very accurate estimates of the modal parameters (natural frequencies, damping ratios, and mode shapes) in the case of noise free input-output data or low output noise. The bias and variance of the modal parameter estimates increase with the level of output noise and with vibration mode order (due to the lower participation of higher modes to the total response and weak signal-to-noise ratio in the application example considered). Both bias and variance of the modal damping ratio estimates are significantly larger that those of the corresponding modal frequency estimates as expected from the system identification literature. In summary, application of GRA is recommended for realization of linear dynamic systems subjected to short-duration and/or non-broadband excitations such as earthquake and shake table excitations when information about the input is available.

ACKNOWLEDGEMENTS

Support of this research by the National Science Foundation, Grant No. DMI-0131967, under a Blue Road Research STTR Project on which UCSD was the principal subcontractor is gratefully acknowledged. Any opinions, findings, and conclusions or recommendations expressed in this material are those of the authors and do not necessarily reflect those of the National Science Foundation.

REFERENCES

Alvin, K. F., Robertson, A. N., Reich, G. W., and Park, K. C. (2003). “Structural system identification: from reality to models.” *Comput. Struct.*, 81(12), 1149–1176.

Caughey, T. H., and O'Kelly, M. E. J. (1965). “Classical normal modes in damped linear dynamic systems.” *J. Appl. Mech.*, ASME, 32, 583-588.

De Callafon, R. A. (2003). “Estimating parameters in a lumped parameter system with first principle modeling and dynamic experiments.” *Proc., 13th IFAC Symposium on System Identification*, Rotterdam, the Netherlands, 1613-1618.

Moaveni, B., De Callafon, R. A., and Conte, J. P. (2007). *General Realization Algorithm for Modal Identification of Linear Dynamic Systems*. Report No. SSRP-07/18, Department of Structural Engineering, University of California, San Diego.

Franklin, G. F., Powel, J. D., and Workman, M. (1998). *Digital control of dynamic systems*, 3rd Ed., Addison-Wesley, Boston, Massachusetts.

Gilbert, E. G. (1963). “Controllability and observability in multivariable control systems.” *SIAM J. Control*, 1(2), 128-151.

Ho, B. L., and Kalman R. E. (1966). “Effective construction of linear state-variable models from input-output functions.” *Regelungstechnik*, 14(12), 545-592.

James, G. H., Carne, T. G., and Lauffer, J. P. (1993). *The natural excitation technique for modal parameters extraction from operating wind turbines.* SAND92-1666, UC-261, Sandia National Laboratories, Sandia, New Mexico.

Juang, J. N., and Pappa, R. S. (1985). “An eigensystem realization algorithm for model parameter identification and model reduction.” *J. Guidance Control Dyn.*, 8(5), 620-627.

Juang, J. N., Cooper J. E. and Wright J. R. (1988). “An eigensystem realization algorithm using data correlations (ERA/DC) for model parameter identification.” *Control Theory Adv. Technol.,* 4(1), 5-14.

Kalman, R. E. (1963). “Mathematical description of linear dynamical systems.” *SIAM J. Control,* 1(2), 152-192.

Kung, S. Y. (1978). “A new identification and model reduction algorithm via singular value decomposition.” *Proc., 12th Asilomar Conference on Circuits, Systems and Computers,* Pacific Grove, USA, 705-714.

Ljung, L. (1999). *System identification: theory for the user,* 2nd Ed., Prentice-Hall, Englewood Cliffs, New Jersey.

Lus, H., Betti, R., and Longman, R. W. (1999). “Identification of linear structural systems using earthquake induced vibration data.” *Earthquake Eng. Struct. Dyn.*, 28(11), 1449-1467.

Lus, H., Betti, R., and Longman, R. W. (2002). “Obtaining refined first order predictive models of linear structural systems.” *Earthquake Eng. Struct. Dyn.,* 31(7), 1413–1440.

Noble, B., and Daniel, J. W. (1988). *Applied Linear Algebra*, 2nd Ed., Prentice Hall, Englewood Cliffs, New Jersey.

Oppenheim, A. V., and Schafer R. W. (1989). *Discrete-time signal processing,* Prentice Hall, Englewood Cliffs, New Jersey.

Peeters, B., and De Roeck, G. (2001). “Stochastic System Identification for Operational Modal Analysis: A Review.” *Journal of Dynamic Systems, Measurements and Control,* 123(4), 659-667.

Peng, B. F., and Conte, J. P. (1998). “Closed-form solutions for the response of linear systems to fully nonstationary earthquake excitation.” *Journal of Engineering Mechanics,* ASCE, 124(6), 684-694.

Phan, M., Horta, L. G., Juang, J.-N., and Longman, R. W. (1992). *Identification of linear systems by an asymptotically stable Observer.* NASA Technical Paper TP-3164, Langley Research Center, Hampton, Vir-

ginia.

Phan, M., Juang, J. N., and Longman, R. W. (1991). *On Markov parameters in system identification*. NASA Technical Memorandum 104156, Langley Research Center, Hampton, Virginia.

Silverman, L. M. (1971). “Realization of linear dynamical systems.” *IEEE Trans. Automat. Control*, AC-16(6), 554-567.

Van Overschee, P., and de Moor, B. (1996). *Subspace identification for linear systems*, Kluwer Academic Publishers, Massachusetts, USA.

Vandewalle, J., and de Moor, B. (1988). “On the use of the singular value decomposition in identification and signal processing.” *Proc. of the workshop of the NATO Advanced Study Institute on Numerical Linear Algebra, Digital Signal Processing and Parallel Algorithms*, Leuven, Belgium, 321-360.

Veletsos, A. S., and Ventura, C. E. (1986). “Modal analysis of non-classically damped linear systems.” *Earthq. Engng. Struct. Dyn*., 14(2), 217-243.

Table 1: Modal parameters of shear building structure

	Mode 1	Mode 2	Mode 3	Mode 4	Mode 5	Mode 6	Mode 7	Mode 8
Undamped frequency [Hz]	1.175	3.484	5.675	7.673	9.409	10.825	11.873	12.516
Pseudo-undamped frequency [Hz]	1.176	3.486	5.687	7.674	9.406	10.871	12.012	12.278
Damped frequency [Hz]	1.175	3.473	5.675	7.662	9.388	10.859	11.977	12.251
Damping ratio [%]	3.77	8.54	6.5	5.65	6.12	4.71	7.68	6.65

Table 2: Statistics of modal parameters identified using GRA based on 100 identification trials at 1% noise level

	Identified-to-exact natural frequency ratio				Identified-to-exact modal damping ratio			
	mean	cov [%]	min	max	mean	cov [%]	min	max
Mode 1	1.000	0.00	1.000	1.000	1.000	0.05	0.998	1.001
Mode 2	1.000	0.01	1.000	1.000	1.000	0.15	0.995	1.003
Mode 3	1.000	0.01	1.000	1.000	1.000	0.23	0.995	1.007
Mode 4	1.000	0.06	0.999	1.005	1.003	0.64	0.989	1.034
Mode 5	1.001	0.13	0.998	1.009	1.020	1.92	0.971	1.084
Mode 6	1.003	0.20	0.995	1.007	1.037	4.33	0.932	1.132

Table 3: Mean and coefficient-of-variation (cov) of MAC values between identified and exact mode shapes based on 100 identification trials at different noise levels

	Mode 1		Mode 2		Mode 3		Mode 4		Mode 5		Mode 6	
	mean	cov [%]	mean	cov [%]	mean	cov [%]	mean	cov [%]	mean	cov [%]	mean	cov [%]
no noise	1.000	0.00	1.000	0.00	1.000	0.00	1.000	0.00	1.000	0.00	1.000	0.00
0.5% noise	1.000	0.03	0.997	0.39	0.991	1.25	0.978	2.96	0.966	4.20	0.903	10.80
1% noise	1.000	0.03	0.997	0.38	0.990	1.27	0.976	3.06	0.959	4.42	0.901	7.35
1.5% noise	1.000	0.03	0.997	0.38	0.990	1.28	0.976	2.99	0.948	4.36	0.860	4.43
2% noise	1.000	0.03	0.997	0.40	0.988	1.31	0.970	3.11	0.937	4.13	0.827	5.78
2.5% noise	1.000	0.03	0.997	0.40	0.988	1.31	0.969	3.14	0.929	4.13	0.818	5.02
3% noise	1.000	0.04	0.997	0.40	0.988	1.31	0.970	3.14	0.922	4.14	0.803	5.61
3.5% noise	1.000	0.04	0.997	0.40	0.988	1.31	0.968	3.15	0.908	4.35	0.780	6.54
4% noise	1.000	0.03	0.997	0.40	0.989	1.31	0.968	3.10	0.888	4.49	0.741	8.98

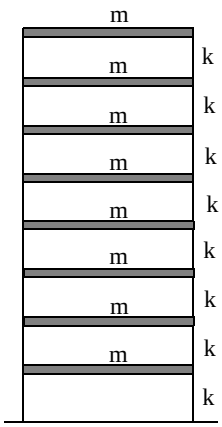

Fig. 1 Eight story shear building model

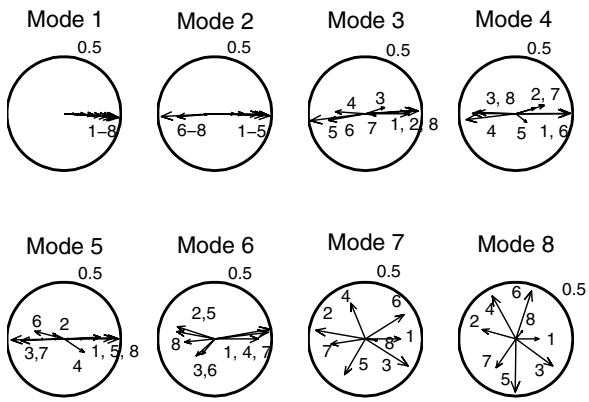

Fig. 2 Polar plot representation of complex mode shapes

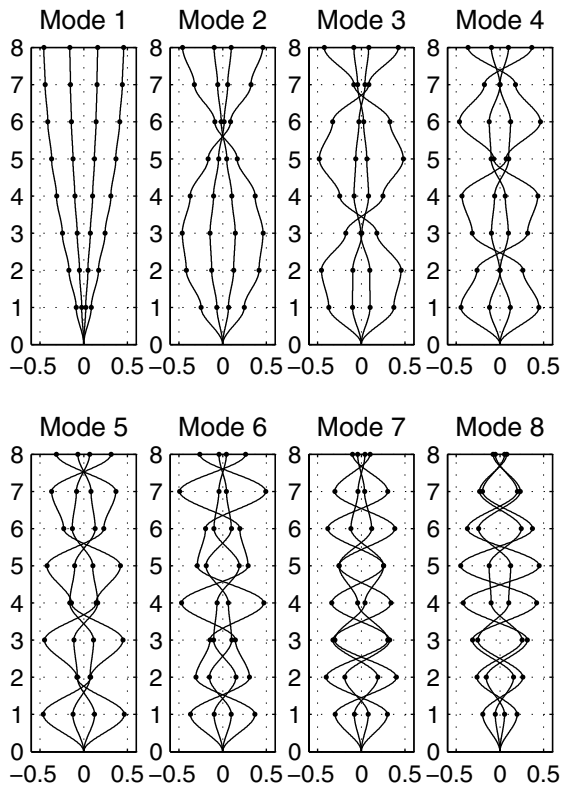

Fig. 3 Exact complex mode shapes of the non-classically damped shear building shown at different phases $(0, \pi/2, \pi, 3\pi/2)$

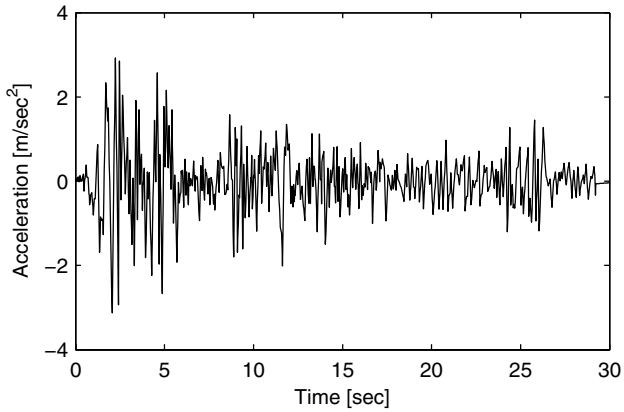

Fig. 4 Imperial Valley, El Centro 1940 earthquake ground motion record

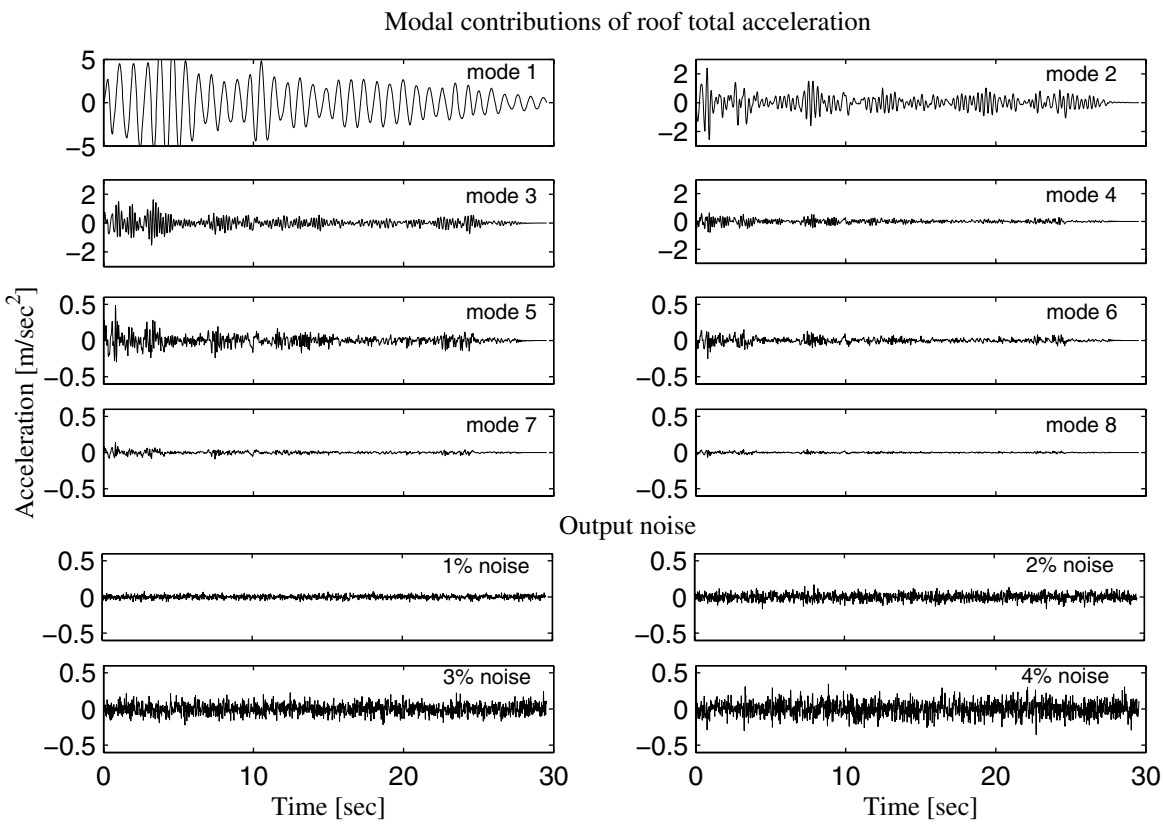

Fig. 5 Modal contributions of total acceleration response at roof level and different levels of added noise

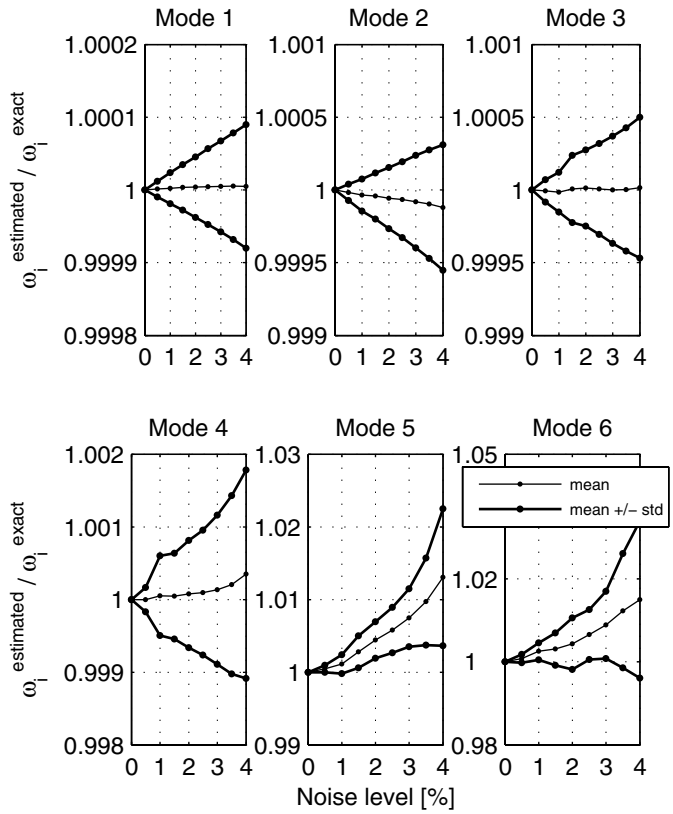

Fig. 6 Statistics of identified-to-exact modal frequency ratios as a function of measurement noise level

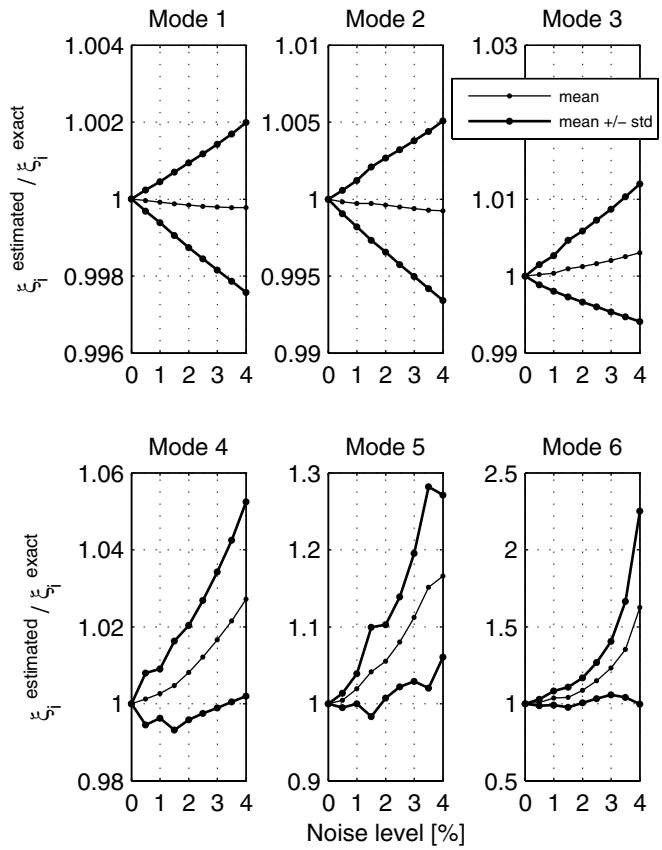

Fig. 7 Statistics of identified-to-exact modal damping ratios as a function of measurement noise level

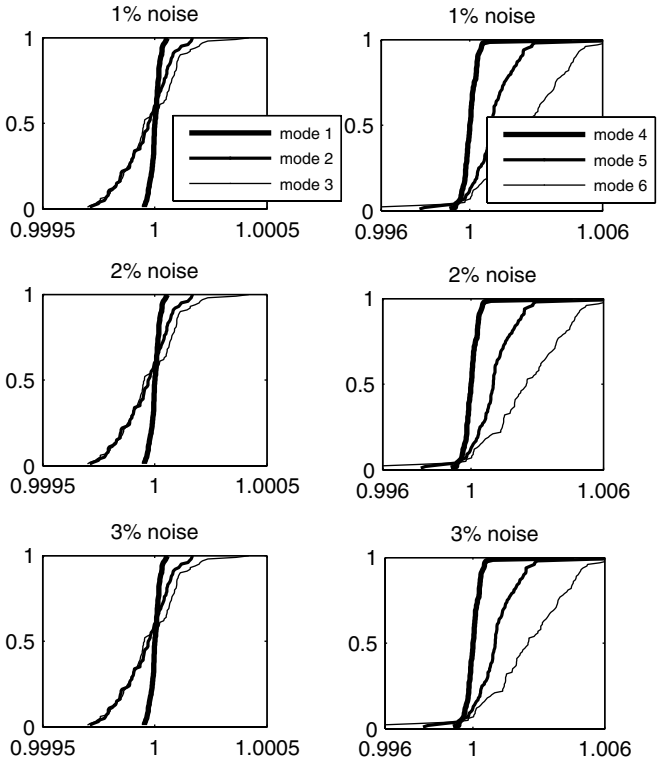

Fig. 8 Cumulative histogram of identified-to-exact modal frequency ratios based on 100 identification trials at noise levels of 1%, 2%, and 3%

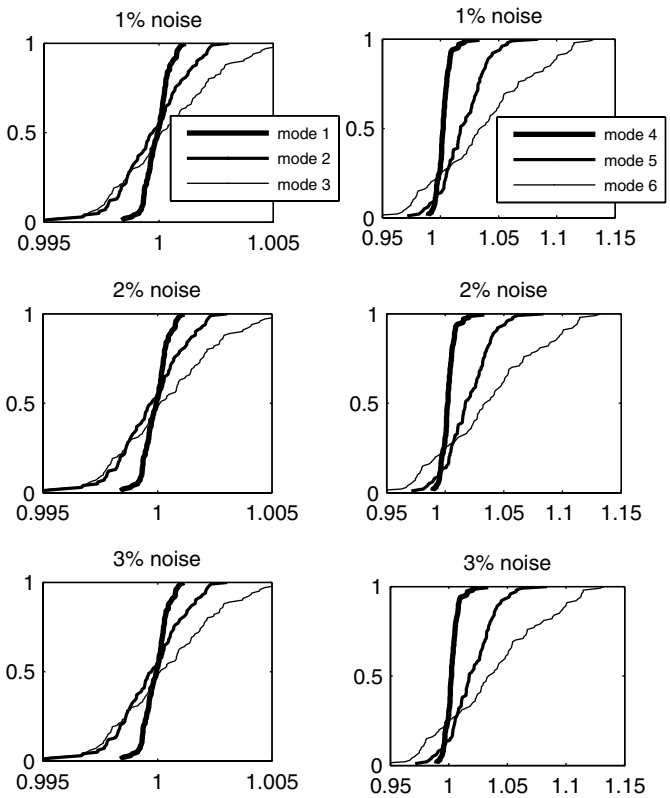

Fig. 9 Cumulative histogram of identified-to-exact modal damping ratios based on 100 identification trials at noise levels of 1%, 2%, and 3%

LIST OF FIGURES

Fig. 1 Eight story shear building model

Fig. 2 Polar plot representation of complex mode shapes

Fig. 3 Exact complex mode shapes of the non-classically damped shear building shown at different phases

Fig. 4 Imperial Valley, El Centro 1940 earthquake ground motion record

Fig. 5 Modal contributions of total acceleration response at roof level and different levels of added noise

Fig. 6 Statistics of identified-to-exact modal frequency ratios as a function of measurement noise level

Fig. 7 Statistics of identified-to-exact modal damping ratios as a function of measurement noise level

Fig. 8 Cumulative histogram of identified-to-exact modal frequency ratios based on 100 identification trials at noise levels of 1%, 2%, and 3%

Fig. 9 Cumulative histogram of identified-to-exact modal damping ratios based on 100 identification trials at noise levels of 1%, 2%, and 3%